Fast calibration methods using cosmic rays for a neutron detection array*

YANG Zai-Hong(杨再宏) YE Yan-Lin(叶沿林)[1)] XIAO Jun(肖军)
YOU Hai-Bo(游海波) LIU HONG-Na(刘红娜) SUN Ye-Lei(孙叶磊)
WANG Zi-Heng(王子蘅) CHEN Jie(陈洁)

School of Physics and State Key Laboratory of Nuclear Physics and Technology, Peking University, Beijing 100871, China

Abstract: An overall irradiation and calibration technique was introduced and applied to a test scintillation detector array. An integral conversion method was used to reduce the nonlinearity of the time difference spectrum, and to improve the position determination especially for positions close to the two ends of a long scintillation bar. An overall position resolution of about 3.0 cm (FWHM) was extracted from the residual analysis method and verified by a direct measurement. Energy calibration was also realized by selecting cosmic rays at different incident angles. The bulk light attenuation lengths for the four test bars were also determined. It is demonstrated that these methods are especially efficient for calibrating large and complex detector arrays.

Key words: neutron detector, calibration, position resolution, deposited energy, bulk light attenuation length

PACS: 21.10.Gv, 29.30.Hs, 29.40.Mc **DOI:** 10.1088/1674-1137/36/3/006

1 Introduction

For extremely neutron-rich nuclei near the neutron drip line, the separation energies of valence neutrons become very small, allowing them to tunnel into the classically forbidden region with a large possibility of forming a so-called "halo" structure [1, 2]. These neutron halo nuclei are often described as an inert core surrounded by several valence neutrons with a large spatial extension [3, 4]. For two neutron halo nuclei, such as ^{11}Li [5–10] and ^{6}He [10–14], the Borromean phenomenon might happen, which means a bound three-body system with all binary subsystems unbound [10]. It is evident that the interaction between the core and the valence neutrons must be nonlinear [4, 10, 15, 16] in order to build this Borromean configuration. So far much attention has been paid to investigating the correlation between the valence neutrons [17–21], but its properties are still not clear. To extract the property of this correlation information from experiments [22, 23], neutron detectors with an excellent performance are crucial, including accurate position and timing resolutions, high detection efficiency and good cross-talk rejection capability [24, 25].

To achieve these requirements, many neutron detector arrays, such as LAND at GSI [26] and MoNA at NSCL [27, 28], have been developed. According to the needs of the next generation of experiments, we are also designing and developing a Multi-neutron Correlation Spectrometer (MunCoS) array, aiming at a horizontal position resolution of less than 5 cm (FWHM) and a timing resolution of less than 800 ps (FWHM). It consists of 80 scintillation bars (type BC-408), each measuring 200 cm×5 cm×6 cm and connected to two photo-multiplier tubes (PMT, type Hamamatsu R1828-01) at each end.

Traditionally the calibration of a large size system relies on some small trigger detectors. Generally it is necessary to move the trigger detectors to many test positions in order to build the distributions. This is quite time consuming and sometimes even impossible if the array structure is complex. Here we introduce an overall irradiation and calibration (OIC) technique

Received 5 July 2011

* Supported by National Natural Science Foundation of China (10827505, 11035001, 10775003, 10905002) and National Basic Research Program of China (2007CB815002)

1) E-mail: yeyl@pku.edu.cn

[26], which is much faster and more effective for a multi-layer large size position sensitive system, such as MunCos. This technique relies on recording all particles passing through the multi-layer system, without position restriction. Then the data are analyzed by applying various conditions as described below. This technique is valid only for systems with good homogeneity and the quality of the results depends on the performance of the overall position resolution.

The test setup is a standing frame which can support up to six (actually only four are used) scintillation bars with a vertical spacing of 17.0 cm to each other. Cosmic ray muons with high energies of a few GeV are used in the test experiment. For each hit on a scintillation bar, timing $t_{\rm L}$ ($t_{\rm R}$) and signal charge $Q_{\rm L}$ ($Q_{\rm R}$) (proportional to the deposited energy) are recorded from the left (right) end of the bar.

The horizontal position along the bar is determined by the difference of the two timing signals taken from both ends, subsequently called "time difference".

2 Position determination

The position y along a scintillation bar is calculated from the time difference (Δt) of the two signals taken from photomultipliers on both ends. The relation is generally expressed by a linear function [26–28]:

$$y = k\Delta t + b. \tag{1}$$

Normally the calibration can be obtained by placing and moving a collimated gamma-ray source along the bar, and recording the time difference accordingly. This traditional method is inefficient and time consuming for a large array like MunCos.

An alternative method has been used in this study [29]. When irradiated by the uniformly distributed cosmic-rays, the time difference spectrum for the whole bar exhibits approximately a rectangular shape with two sharp edges (Fig. 1). Based on the linear relationship between the position and time difference, two edges of the rectangular spectrum correspond to the geometrical two ends of the bar and then this linear relationship can be deduced by accurately determining the spectrum edges.

A differential operation is applied to the time difference spectrum. The two peak positions of the differential spectrum are accepted as corresponding to the two edge positions of the bar ($B_{\rm U}$ and $B_{\rm D}$). The linear relationship between the position y (in cm) along the bar and the time difference Δt can then be expressed as:

$$y = \frac{\Delta t - B_{\rm D}}{B_{\rm U} - B_{\rm D}} L. \tag{2}$$

or as a linear function of Δt:

$$y = \frac{L}{B_{\rm U} - B_{\rm D}} \Delta t - \frac{L B_{\rm D}}{B_{\rm U} - B_{\rm D}}. \tag{3}$$

where L (in cm) is the length of the bar. This overall measurement is obviously much faster than the usual collimation measurement.

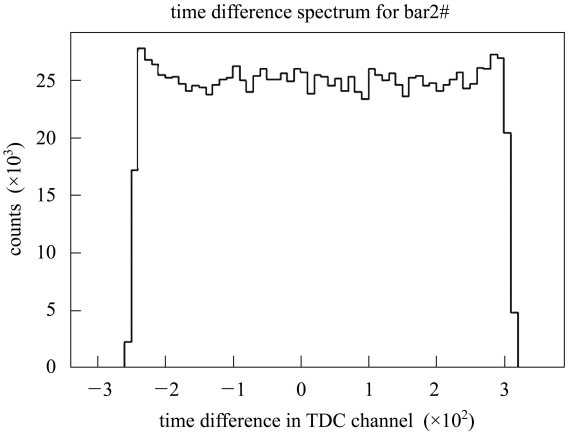

Fig. 1. Time difference spectrum for bar2#, expressed in TDC channels.

The above method is used for a linear interpretation. But as we can see from Fig. 1, some nonlinearity appears along the distribution, especially around the two edges. From the uniform irradiation assumption, these nonlinearities might be corrected. Denoting ϕ the average count rate per unit length, the integral count (ΔN) on a given length interval (ΔL) can be expressed as: $\Delta N = \Delta L \phi$. ϕ might be obtained from the total count ($N_{\rm t}$) of the whole bar as $\phi = N_{\rm t}/L$. The actual position y relative to the left end, for a given time difference value (Δt), is now determined by the integral spectrum $N(\Delta t)$:

$$y = \frac{N(\Delta t)}{\phi} = \frac{N(\Delta t)}{N_{\rm t}} L. \tag{4}$$

where both Δt and $N(\Delta t)$ are counted from the left end to the actual value.

The integral function $N(\Delta t)$ can be determined from the time difference spectrum in Fig. 1 and the position y for each Δt can then be deduced, as illustrated in Fig. 2. Once the y versus Δt relation is fixed through this integral conversion (IC) method as demonstrated in Fig. 2, it can be applied to arbitrary irradiation cases to build realistic position spectra.

In order to verify the validity of this IC method, two 3-cm-wide small trigger scintillators were placed

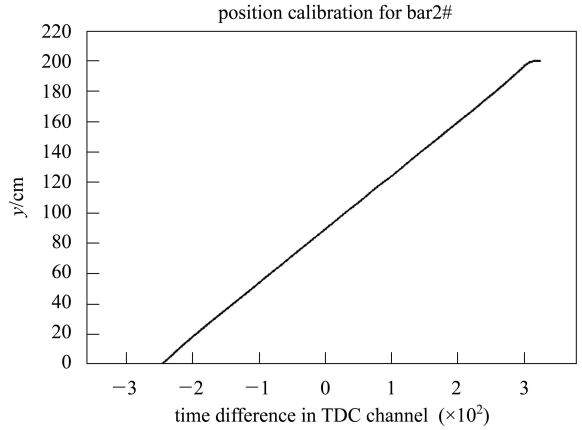

Fig. 2. The position y for each Δt from the integral conversion (IC) method.

above the scintillation bar and centered at 70.0 cm and 130.0 cm, successively, from the left end of the bar. The measured time difference spectrum was converted to the position spectrum according to the above described IC method, as shown in Fig. 3. Gaussian fits to the peaks reproduce very well the manually set positions, proving the validity of the IC method.

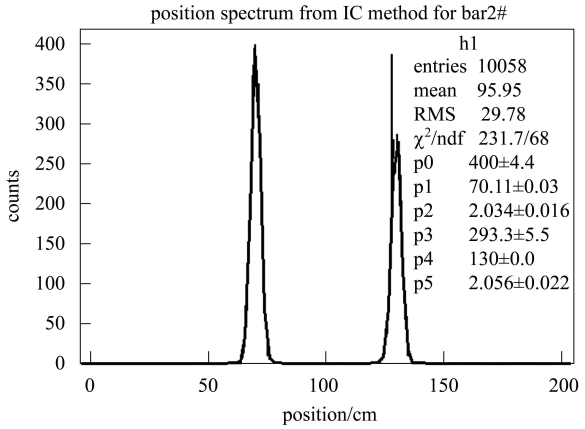

Fig. 3. Position spectrum of the cosmic rays triggered by two small scintillators for bar2#. The position spectrum was converted from the time difference spectrum according to the IC method. The manually set trigger positions (centered at 70.0 and 130.0 cm from the left end of the bar) are well reproduced (70.11±0.03 cm and 130.0±0.0 cm, respectively, based on the Gaussian function fits).

This IC method is especially useful to correct the nonlinearity near the two ends of a bar, where the light propagation speed varies dramatically, and the linear Eq. (1) is no longer valid. The difference between the positions determined from the IC method ($y_{\rm IC}$) and from the linear formula ($y_{\rm LF}$) is shown in Fig. 4. To avoid meaningless long tails, time difference spectrum cut offs were applied around the values corresponding to the geometrical ends of the bar. As can be seen from Fig. 4, the deviation in the central part of the bar is less than about 0.2 cm, arising basically from statistical fluctuations, while large deviations appear near the two ends. It is clear that the IC method improves largely the position determination in these regions.

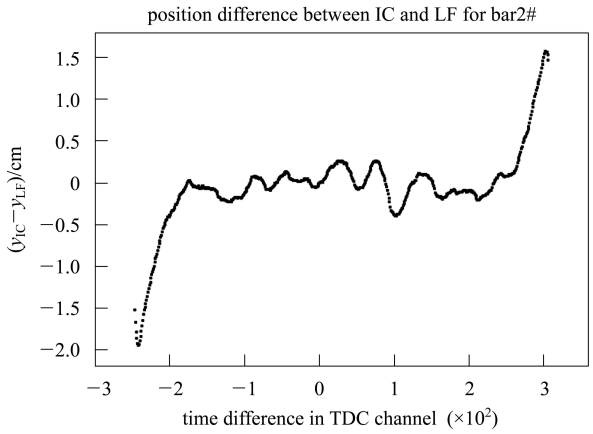

Fig. 4. The difference between the position determined from the IC method and that from the linear formula (LF).

In a cosmic ray test of a multi-bar array, a muon may simultaneously penetrate several bars and even fire all of them. To determine a track correctly, the whole system must be aligned along the y dimension and the offsets should be fixed for every bar. Normally the uppermost and the lowest bars are manually aligned as accurately as possible to serve as reference bars. Then a narrow cosmic ray beam is selected by cutting small position windows on the reference bars. The offset for each test bar can then be fixed by shifting the measured spectrum position to match the reference bar position.

3 Position resolution

Normally a very small collimated radiation source is needed to determine the position resolution. Here we use, as an alternative, a much faster approach [26] relying on the measurement of all cosmic-ray tracks passing through the whole system. For each coincidentally recorded event, a straight line can be obtained by a linear fit to the four hitting points on the four bars. Then the distance between the actual measured position and the fitted hitting position is recorded for each bar as its residual. This procedure is repeated for all measured tracks, regardless of their

actual position on the bar. A residual spectrum for each bar can then be accumulated. One example is plotted in Fig. 5. This kind of residual spectrum is a description of the performance of position determination [26]. According to a Monte Carlo simulation for the current detector setup [29], the position resolution should be about 1.25 times the residual uncertainty. From this "residual analysis" (Fig. 5), the position resolution (FWHM) of bar2# is extracted to be about 3.0 cm.

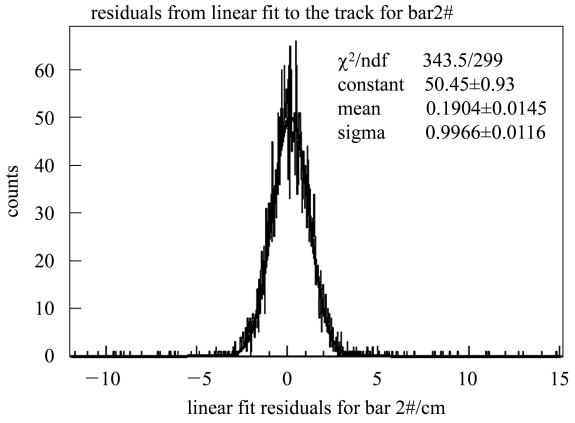

Fig. 5. The accumulated residual spectrum, as defined in Section 3, for bar2#. A Gaussian function fit gives a standard deviation of 1.00±0.01 cm.

The above determined position resolution might be verified by the traditional direct measurement method. Using the triggered test data shown in Fig. 3, a standard deviation of about 2.05 cm is obtained, including contributions from the finite size of the trigger scintillator and the resolution of the bar itself. After subtracting the former by a Monte Carlo simulation, the position resolution (FWHM) was determined to be around 3.2 cm, which agrees well with the residual analysis. Therefore in cases where direct measurement is not applicable (for a complex and large array for instance), residue analysis would provide a timely and effective way to check the position resolution.

4 Calibration of the deposited energy

Energy deposited in a scintillation bar is a critical quantity for particle identification and for neutron cross-talk rejection [30]. A new approach with various path lengths of the cosmic rays was applied in our test experiment. For each event, the charges of the left and right side PMT signals, $Q_{\rm L}$ and $Q_{\rm R}$, are recorded by a Charge-to-Digit-Converter (QDC). For a long straight bar the exponential law for attenuation of the light signal charge along the bar is well satisfied [31]. Therefore the position independent geometric mean charge Q for each event can be calculated from $Q_{\rm L}$ and $Q_{\rm R}$ as:

$$Q=\sqrt{Q_{\rm L}Q_{\rm R}}. \tag{5}$$

Generally, Q is proportional to the deposited energy ΔE:

$$Q=a\Delta E+b. \tag{6}$$

The coefficients a and b for a limited energy range can be calibrated by using cosmic-ray muons at different incident angles, corresponding to different path lengths. Denoting θ the incident angle, $\dfrac{{\rm d}E}{{\rm d}x}$, the energy loss of the incident particle (muon here) per unit length and h the thickness of the bar, we have:

$$Q=a\left(-\frac{{\rm d}E}{{\rm d}x}\right)\frac{h}{\cos\theta}+b=\frac{C}{\cos\theta}+D, \tag{7}$$

with

$$C=a\left(-\frac{{\rm d}E}{{\rm d}x}\right)h$$

and $D=b$, both being constants. Data used in the above sections are from the same test measurement. They can also be used here to determine C and D. Since all scintillation bars are position sensitive as described above, tracks with incident angles from 0 to 60 degrees can be selected for the calibration. For each 5° angular interval, Q values (in channel) of the events are accumulated, and the mean Q value for this interval is obtained from a Landau function fit to the distribution. Shown in Fig. 6 are the mean Q values versus $1/\cos\theta$, where θ is taken as the mean angle of the corresponding angular interval. A linear fit is also displayed in the figure together with the

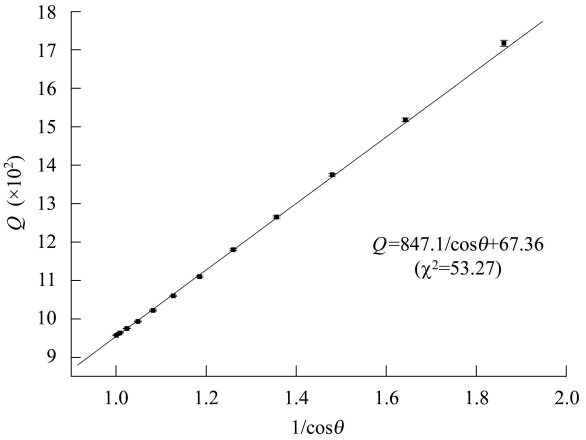

Fig. 6. Linear relationship between the signal charge Q (in channel) and $1/\cos\theta$ for bar2#. Similar results were also obtained for other three test bars.

obtained parameters. The absolute value of $\mathrm{d}E/\mathrm{d}x$ is 2.0 MeV ee (electron equivalent energy) /(g/cm^2) for high energy cosmic muons passing through a plastic scintillation counter [32]. With a density of 1.032 g/cm^3 and a thickness of 5 cm for a current scintillation bar, constant a (in Channel/MeV ee) in Eq. (6) for the current test bar2# can be deduced as: $a = C/10.32$ MeV ee=82.1 ch/MeV ee. And constant b is equal to D (67.4 Channels), corresponding to the background level.

5 Bulk light attenuation length

The bulk light attenuation length is an important parameter describing the performance of a long scintillation bar. This parameter can also be determined by the OIC method. When a muon hits a scintillation bar at position y (relative to the left end), two light signals will propagate to the left and right ends, respectively. The signals will be attenuated exponentially along their paths, and be collected and converted to charge signals by PMTs. The charge signals for the PMTs, in QDC channels, are then expressed as:

$$Q_{\mathrm{L}} = c_{\mathrm{L}} E_{\mathrm{L}} \mathrm{e}^{\frac{-y}{\lambda}} \qquad Q_{\mathrm{R}} = c_{\mathrm{R}} E_{\mathrm{R}} \mathrm{e}^{\frac{-(L-y)}{\lambda}}, \qquad (8)$$

where c_{L} and c_{R} are the PMT response coefficients, E_{L} and E_{R} the light sharing at the position of track crossing, and λ the bulk light attenuation length. We further deduce:

$$\begin{aligned} \ln(Q_{\mathrm{R}}/Q_{\mathrm{L}}) &= \ln(E_{\mathrm{R}}/E_{\mathrm{L}}) + \ln(c_{\mathrm{R}}/c_{\mathrm{L}}) + (2x-L)/\lambda \\ &= M + (2/\lambda)y, \end{aligned} \qquad (9)$$

with $M = \ln(E_{\mathrm{R}}/E_{\mathrm{L}}) + \ln(c_{\mathrm{R}}/c_{\mathrm{L}}) - L/\lambda$, being independent of position y.

All recorded events with hitting positions in a range between 30 cm and 170 cm are used and divided into y intervals of 10 cm each. For each position interval, $\ln(Q_{\mathrm{R}}/Q_{\mathrm{L}})$ values are accumulated, and their mean value is obtained from a Gaussian function fit to the distribution of $\ln(Q_{\mathrm{R}}/Q_{\mathrm{L}})$. In Fig. 7, the averaged $\ln(Q_{\mathrm{R}}/Q_{\mathrm{L}})$ results are plotted against the interval mean positions, and a good linear relationship is obtained. Attenuation length λ can then be extracted from fitting the data with Eq. (9).

Results for the current four test bars are listed in Table 1. The error bars on the data points in Fig. 7 with the parameters in Table 1 are statistical only. Due to light reflection processes within a limited bar volume, the realistic attenuation lengths in Table 1 are normally smaller than those in an infinitely large size crystal, namely 380 cm given by the manufacturer (Saint-Gobain Crystals). Also the attenuation length varies bar to bar, as indicated in the table, due to possibly the non-uniformity of the crystal property and the treatment of the crystal surface.

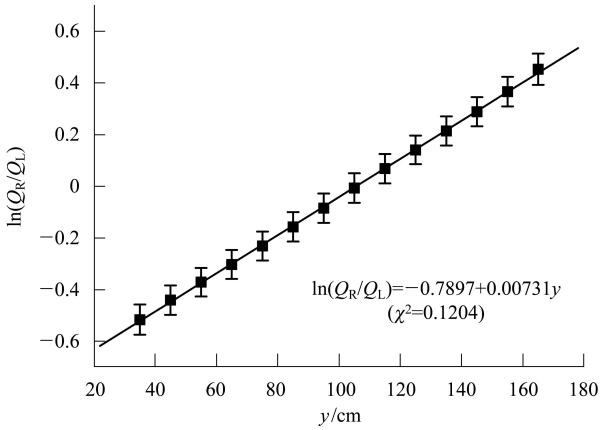

Fig. 7. $\ln(Q_{\mathrm{R}}/Q_{\mathrm{L}})$ as a function of the position along the scintillation bar0#. Similar results were also obtained for other three test bars.

Table 1. The bulk light attenuation length (λ) for each test bar, determined from the present test experiment.

bar	#0	#1	#2	# 3
λ/cm	273.6±1.4	255.9±0.7	338.6±2.8	321.9±2.5

6 Summary

An overall irradiation and calibration technique was developed and applied to determine the detection performances of a scintillation detector array. All cosmic ray muons passing through the whole system were recorded simultaneously and contribute equally to the calibration procedure. Based on a large number of events the test procedure becomes fast and very effective. Through a differential operation on the time difference spectrum, the channels corresponding to the geometrical two ends of the bar are precisely determined. An integral conversion method can be used to reduce the nonlinearity of the time difference spectrum, and to improve the position determination, especially when approaching the end of a bar. An overall position resolution of about 3.0 cm (FWHM) was extracted from the residual analysis and verified by a direct measurement. Energy calibration was realized by using cosmic-rays at different incident angles. The bulk light attenuation lengths for the four test bars are also obtained. Techniques and methods developed here are applicable to other multi-layer large-size position-sensitive arrays.

References

1 Hansen P G. Nucl. Phys. A, 1989, **553**: 89–106
2 Pougheon F. Z. Phys. A, 1994, **349**: 273–278
3 Jonson B. Phy. Rep, 2004, **389**: 1–59
4 Jensen A S, Riisager K, Fedorov D V. Rev. Mod, 2004, **76**: 215–261
5 Tanihata I, Hamagaki H, Hashimoto O et al. Phys. Rev. Lett., 1985, **55**: 2676
6 Kobayashi T, Yamakawa O, Omata K et al. Phys. Rev. Lett., 1988, **60**: 2599
7 Shimoura S, Nakamura T, Ishihara M et al. Phys. Lett. B, 1995, **348**: 29–34
8 Nakamura T, Vinokumar A M, Sugimoto T et al. Phys. Rev. Lett., 2006, **96**: 252502
9 Ieki K, Sackett D, Galonsky A et al. Phys. Rev. Lett., 1993, **70**: 730
10 Zhukov M V, Danilin B V, Fedorov D V. Phy. Rep, 1993, **231**: 151–199
11 Cortina-Gil M, Roussel-Chomaz P, Alamanos N et al. Phys. Lett. B, 1997, **401**: 9
12 Alkhazov G D, Andronenko M N, Dobrovolsky A V et al. Phys. Rev. Lett., 1997, **78**: 2313
13 Wang J, Galonsky A, Kruse J J et al. Phys. Rev. C, 2002, **65**: 034306
14 YE Y L, PANG D Y, JIANG D X et al. Phys. Rev. C, 2005, **71**: 014604
15 Ershov S N, Grigorenko L V, Vaagen J S, Zhukov M V. J Phys G, 2010, **37**: 064026
16 Simon H, Meister M, Aumann T et al. Nucl. Phys. A, 2007, **791**: 267–302
17 Hagino K, Sagawa H, Schuck P. J Phys G, 2010, **37**: 064040
18 Tanihata I. J. Phys. G, 1996, **22**: 157
19 Fredericl T, Yamashita M T, Lauro Tomio. Nucl. Phys. A, 2007, **787**: 561c–568c
20 Hagino K, Sagawa H. Phys. Rev. C, 2005, **72**: 044321
21 Hagino K, Sagawa H, Carbonell J et al. Phys. Rev. Lett., 1997, **99**: 022506
22 David H Boal, Claus-Konrad Gelbke, Byron K Jennings. RevModPhys, 1990, **62**: 553–602
23 Marques F M, Labiche M Orr et al. Phys. Lett. B, 2000, **76**: 219
24 Nakamura T, Vinodkumar A M, Sugimoto N A T et al. Phys. Rev. Lett., 2006, **96**: 252502
25 WANG J, Galonsky A, Kruse J J et al. Nucl. Instrum. Methods A, 1997, **397**: 380
26 Blaich Th, Elze Th W, Embling H et al. Nucl. Instrum. Methods A, 1992, **314**: 136–154
27 Luther B, Baumann T, Thoennessen M et al. Nucl. Instrum. Methods A, 2003, **505**: 33–35
28 Baumann T, Boike J, Brown J et al. Nucl. Instrum. Methods A, 2005, **543**: 517–527
29 YANG Zai-Hong, YOU Hai-Bo, XIAO Jun, YE Yan-Lin et al. Plasma Science and Technology, 2011, (accepted)
30 Sackett D, Ieki K, Galonsky A et al. Phys. Rev. C, 1993, **48**: 118–135
31 Grabmayr P, Hehl T, Stahl A et al. Nucl. Instrum. Methods A, 1998, **402**: 85–94
32 Gibelin Julien Search for Low Lying Dipole Strength in the Neutron Rich Nucleus ^{26}Ne (PhD thesis), France: Universite de Paris-Sub, 2005